The Field Displacement Isolator

By S. WEISBAUM and H. SEIDEL

(Manuscript received February 7, 1956)

A nonreciprocal ferrite device (field displacement isolator) has been constructed with reverse to forward loss ratios of about 150 in the region from 5,925 to 6,425 mc/sec. The forward loss is of the order of 0.2 db while the reverse loss is 30 db. These results are obtained by using a single ferrite element, spaced from the sidewall of the guide. The low forward loss suggests the existence of an electric field null at the location of a resistance strip on one face of the ferrite. We discuss the various conditions, derived theoretically, under which the electric field null may be obtained and utilized. Furthermore, a method of scaling is demonstrated which permits ready design to other frequencies.

I. INTRODUCTION

The need for passive nonreciprocal structures has long been recognized.[1] In the microwave field, Hogan's gyrator[2] paved the way for an increasingly important class of such devices. The isolator, in particular, has emerged as one of the more useful ferrite components. It performs the function, as its name implies, of isolating the generator from spurious mismatch effects of the load. Unlike lossy pads, which consume generator power, the isolator provides a unidirectionally low loss transmission path.

A. G. Fox, S. E. Miller and M. T. Weiss[3] have pointed out that nonreciprocal ferrite devices may exploit any of the following waveguide effects:

1. Faraday rotation
2. Gyromagnetic resonance
3. Field displacement
4. Nonreciprocal phase shift

In the present paper we shall discuss an isolator, based upon the field displacement effect, which was developed to meet the following requirements for a proposed microwave relay system (5,925–6,425 mc/sec):

1. Forward loss 0.2 db

2. Reverse loss 20 db
3. Return loss 30 db

The field displacement isolator employs an ordinary rectangular waveguide and requires no specialized adaptation to the rest of the guide system. It is relatively compact and does not require excessive magnetic fields. In contrast to the field displacement structure of Reference 3, in which a symmetrically disposed pair of ferrite slabs is used, the present unit (see Fig. 1) contains only a single slab. Other differences of a more substantial nature may be noted — in the present case the slab is displaced from the guide wall, it occupies a partial height of the waveguide, and it employs a novel disposition of the absorption material on one face. These features result in a broadband device.

In the analysis presented in this paper the isolator field characteristics for a full height slab are determined by exact solution of Maxwell's equations, as opposed to the "point-field" perturbation approximation used in Reference 3. An exact solution of the partial height geometry of the experimental device would be exceedingly difficult to obtain. However, such a solution did not appear to be essential for this investigation since good correspondence has been obtained between the experimental results and the idealized full height slab calculations.

The following performance of the isolator was obtained from 5,925–6,425 mc/sec:

1. Forward loss $\sim$ 0.2 db

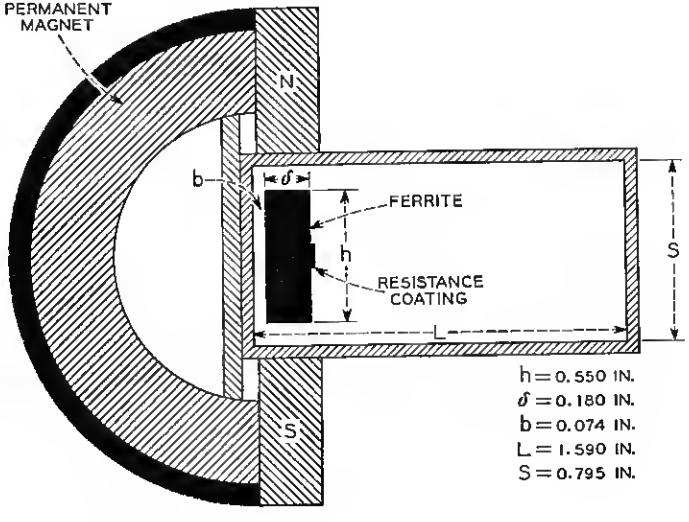

Fig. 1 — Field displacement isolator.

2. Reverse loss $\sim$ 30 db
3. Return loss $\sim$ 30 db

The extremely low forward loss strongly suggested the existence of an electric field null in the plane of the resistance material. Consequently, a theoretical investigation of the null condition was made and a set of criteria established for the existence and utilization of the null. (E. H. Turner[4] independently developed the same null conditions.) An extension of the analysis leads directly to a set of scaling laws which permits the ready design of isolators of comparable performance at other frequency bands.

II. DESCRIPTION OF OPERATION

In Section IIA we will show how the "point-field" approach[3] is used to predict the qualitative behavior of the structure and in Section IIB we will apply a more rigorous analysis to the determination of the optimum design parameters.

A. Qualitative

Prior to introducing the actual isolator configuration, we shall review some elementary properties both of the ferrite medium and of an unloaded rectangular waveguide. It is in terms of these properties that we can understand, in a qualitative sense, the interaction of an *rf* wave with a ferrite in such a waveguide. Since the behavior of a ferrite medium in the presence of a static magnetic field and a small *rf* field has been discussed in the literature[5] the following resumé is not intended to be detailed. It is presented, however, to maintain continuity.

If a static magnetic field is applied to a ferrite medium the unpaired electron spins, on the average, will line up with the field. If now an *rf* magnetic field, transverse to the dc field, excites the spin system these electrons will precess, in a preferential sense, about the static field. The precession gives rise to components of transverse permeability at right angles to the *rf* magnetic field, leading to a tensor characterization of the medium. This tensor has been given by Polder[5] and may be diagonalized in terms of circularly polarized wave components. Corresponding to the appropriate sense of polarization we use the designation $+$ and $-$. When the polarization is in the same sense as the natural precessional motion of the spin system, gyromagnetic resonance occurs for an appropriate value of the static magnetic field. The scalar permeabilities μ_- and μ_+ are shown in Fig. 2 as functions of the internal static magnetic field as would be observed at an arbitrary frequency.

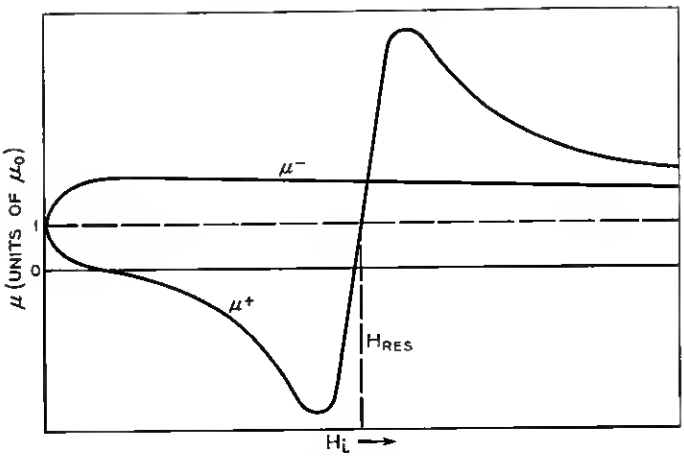

Fig. 2 — Permeability versus magnetic field.

Clearly, in employing a ferrite medium, we intend to use the basic difference between the scalar permeabilities μ_+ and μ_-. To this end we may exploit the fact that the magnetic field configuration at any given point in a rectangular waveguide is, in general, elliptically polarized. Traveling loops of magnetic intensity appear in Fig. 3 for the fundamental (TE_{10}) mode. At point P an observer sees a counterclockwise elliptically polarized magnetic intensity if the wave is traveling in the (+y) direction.* The propagating wave may be decomposed into two oppositely rotating circularly polarized waves of different amplitudes:

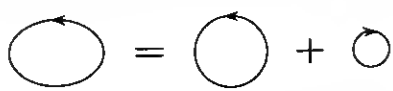

For propagation in the (−y) direction the *rf* polarization is reversed:

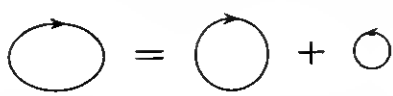

Let us now consider the actual experimental configuration shown in Fig. 4 (the partial height geometry was chosen on an experimental basis, in that it gave VSWR considerably less than that for a full height ferrite slab). The precession of the spin magnetic moments is counterclockwise

* It is evident that a point converse to P exists symmetrically to the right of center. This is utilized in a double slab isolator which has been investigated by S. Weisbaum and H. Boyet, I.R.E., **44**, p. 554, April, 1956.

looking along the direction of the dc magnetic field shown in Fig. 4. Since the major component of circular polarization for $(+y)$ propagation is also counterclockwise the permeability will be less than unity for this direction of propagation. This occurs provided we are using small static fields, as is readily verified from Fig. 2. The permeability will be greater than unity for $(-y)$ propagation. Physically, this is equivalent to energy being crowded out of the ferrite for $(+y)$ propagation and to energy being crowded in, in the reverse direction. The electric field will thus be distorted as shown in a qualitative way in Fig. 5. The vertical dimension in this figure serves both to identify the guide configuration and to provide an ordinate for the electric field intensity.

The fields as shown in Fig. 5 merely represent a qualitative picture of the distributions in the guide and are not intended to be exact. There is no question, however, that the electric fields at the ferrite face are dif-

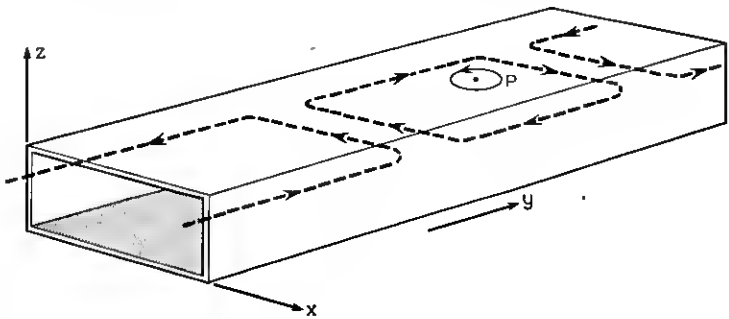

Fig. 3 — Magnetic field configuration — Dominant TE_{10} mode.

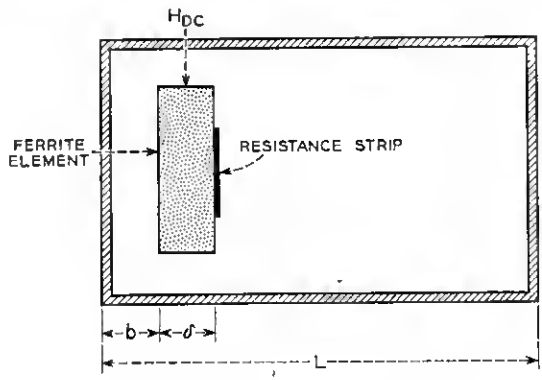

Fig. 4 — Experimental configuration.

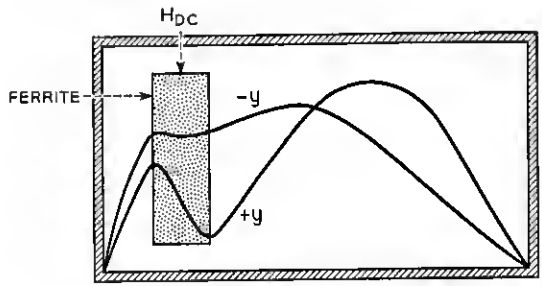

Fig. 5 — Electric field distortion.

ferent in magnitude corresponding to the two directions of propagation. Hence, if resistance material is placed at the interior face of the ferrite (see Fig. 1) we may expect to absorb more energy in one direction of propagation.

B. Analysis of Electric Field Null:-Full Height Ferrite

The description we have given in Section IIA is based on a perturbation approach and does not take into account the higher order interaction effects of the ferrite and the propagating wave. In this section we consider an analysis of the idealized case, namely that of a full height ferrite slab, and impose the condition of an electric field null at the face of the ferrite for the forward direction of propagation. While this too does not represent the true experimental situation, we believe it to be a better approximation than the "point-field" perturbation viewpoint.

The fields of the various regions shown in Fig. 6 are described as follows:

$$E_z^{(1)} = \sin \alpha_1 x$$
$$E_z^{(2)} = Ae^{-i\alpha_2 x'} + Be^{i\alpha_2 x'} \quad \text{where} \quad x' = x - a \qquad \text{(II — 1)}$$
$$E_z^{(3)} = V \sin \alpha_1 x'' \quad \text{where} \quad x'' = x - L$$

where

α_j = transverse wave number in the j^{th} region
a = transverse dimension from narrow wall to ferrite face
L = broad waveguide dimension
x = variable dimension along broad face
z = height variable
A, B, V = constants

Setting up the wave equation, there results

$$\alpha_2^2 = K^2\left[\frac{\varepsilon_r}{\mu_r}(\mu_r^2 - k_r^2) - 1\right] + \alpha_1^2 \qquad \text{(II—2)}$$

where μ_r and k_r are the relative diagonal and off-diagonal terms of the Polder tensor, respectively, K is the free space wave number and ε_r is the relative dielectric constant.

$$\mu_r = 1 + \frac{4\pi M_S \gamma \omega_0}{\omega_0^2 - \omega^2}$$

$$k_r = \pm \frac{4\pi M_S \gamma \omega}{\omega_0^2 - \omega^2}$$

$\gamma = 2.8 \times 10^6$ cycles/sec/oersted
$4\pi M_S$ = saturation magnetization in gauss
H_0 = static magnetization in oersteds
$\omega_0 = \gamma H_0$

$$K = \frac{2\pi}{\lambda}$$

The following transcendental equation results from satisfying the boundary conditions on E and H:[6]

$$\frac{\tan \alpha_1 a[\mu_r \alpha_2 + k_r \beta \tan \alpha_2 \delta] + (\mu_r^2 - k_r^2)\alpha_1 \tan \alpha_2 \delta}{(\beta^2 - K^2 \mu_r \varepsilon_r) \tan \alpha_1 a \tan \alpha_2 \delta + \alpha_1(\mu_r \alpha_2 - k_r \beta \tan \alpha_2 \delta)} + \frac{\tan \alpha_1 b}{\alpha_1} = 0 \qquad \text{(II—3)}$$

where β is the propagation constant.

The minimum nontrivial value of α_1 causing a null to appear at the ferrite face is $\alpha_1 = \pi/a$. Placing this value in (II — 3) produces the following transcendental equation for the null:

$$\frac{\frac{\pi}{a}(\mu_r^2 - k_r^2) \tan \alpha_2 \delta}{\mu_r \alpha_2 - k_r \beta \tan \alpha_2 \delta} + \tan \alpha_1 b = 0 \qquad \text{(II—4)}$$

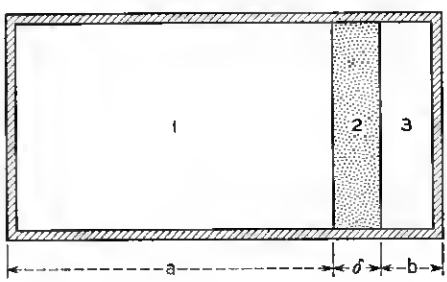

Fig. 6 — Full height geometry.

where $b = L\text{-}a\text{-}\delta$. Equation (II — 4) demonstrates that the null condition is nonreciprocal since, in general, the solutions differ for k_r positive and k_r negative. The quantity k_r has the same sign as the direction of the dc magnetic field; reversing the sign of k_r is equivalent to reversing the direction of propagation.

A numerical analysis of equation (II — 4) has led to the conclusion that the null condition is most broadband when $|\mu_r| < |k_r|$.* We use the criterion $|\mu_r| = |k_r|$ to determine a critical magnetic field:

$$H_c = \frac{\omega}{\gamma} - 4\pi M_S \qquad \text{(II — 5)}$$

Clearly we require $\omega/\gamma > 4\pi M_S$ for physically realizable solutions. The saturation magnetization ($4\pi M_S$) is subject to the following:

1. A choice of too large a $4\pi M_S$ might create a mode problem and in addition will not satisfy the limit on $4\pi M_S$ implied in (II — 5).

2. $4\pi M_S$ must be sufficiently large so that the field needed to make $|\mu_r| < |k_r|$ not be excessive.

3. $\gamma\sqrt{H(H + 4\pi M)}$ (this being the slab resonance frequency for small slab thickness[7]) must be sufficiently far from the operating frequency to avoid loss due to resonance absorption. In addition, this condition improves the frequency insensitivity of the null.

Further analytic considerations are presented in Section IV.

III. EXPERIMENTAL DESIGN CONSIDERATIONS

Aside from the partial height nature of the slab, there are two other basic factors in the experimental situation which are not present in the analysis of Section IIB (see also Section IV). First, the ferrite has both finite dielectric and magnetic loss. Second, higher order modes may be present. These deviations from the simplified analysis are by no means trivial and it would not be surprising if one found a considerable modification of the analytic results. As it turns out, there are broad areas of general agreement between the theoretical and experimental results and in no case examined here does one find a basic inconsistency. In considering the various parameters which must be adjusted to optimize the broadband performance of the isolator we will point out, where possible, how the theoretical results are modified by the factors mentioned above. The parameters of interest are:

* This is partially evident from equation II — 4. The quantity $|\mu_r|$ must be less than $|k_r|$ if the angle $(\alpha_i b)$ is to be small and in the first quadrant. Second quadrant solutions cause the guide cross section to be excessively large, with attendant higher mode complication.

A. The saturation magnetization ($4\pi M_s$) and the applied magnetic field (H_{DC}).

B. The ferrite height.

C. The thickness (δ) of the ferrite and its distance (b) from the nearest sidewall.

D. The placement of the resistance material and its resistivity (ρ).

E. The length of the ferrite (ℓ).

A. $4\pi M_s$ and H_{DC}

Theoretically, minimum forward loss occurs with a true null at the face of the loss film and has been given in the condition $|\mu_r| < |k_r|$. Although this inequality is required in the full height slab analysis, experiment (Fig. 7) indicates the low loss region to be so broad as to extend well into the low field, or $|\mu_r| > |k_r|$ region.

There is inherent loss in the ferrite so that a more accurate statement of the bandwidth of operation is that in which the losses in the film are of equal order to the ferrite losses at the band edges. Even discounting ferrite losses, it will be shown in Section IV that we have a good analytic basis for the observed broadness of the low loss region. In general, therefore, we need not be as restrictive as the null analysis of Section IIB would imply. It is not surprising then that optimum operation actually occurs in the region $|\mu_r| > |k_r|$. There are several reasons why this may be so:

1. Shift of operation occurs due to the partial height nature of the ferrite slab.

2. Reverse loss has a peak in the low field region, requiring a compromise of low forward loss and high reverse loss for best isolation ratios (see Fig. 8).

3. Optimum compromise between low ferrite loss and low film loss must be made.

The internal magnetic field, determining $|\mu_r|$ and $|k_r|$, differs from the applied field by the demagnetization of the ferrite slab. Although not ellipsoidal, it may nonetheless be considered to have an average demagnetization which has been computed, for this case, to be 460 oersteds. A further complication in knowledge of the internal field is the proximity effect of the pole pieces. This latter correction was obtained experimentally and, all in all, it was determined that the internal field for optimum operation was of the order of 300 oersteds. For the given ferrite and the range of frequency of operation, this internal field corresponds to the condition that $|\mu_r| > |k_r|$, as stated above.

Taking all effects into account, it was found that optimum permanent magnet design occurred for an air gap field of 660 oersteds.

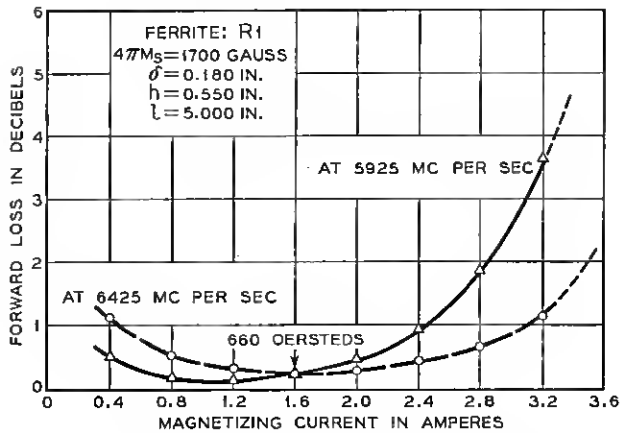

Fig. 7 — Forward loss versus magnetizing current.

Using the experimental values $4\pi M_S$ = 1,700 gauss and internal magnetic field = 300 oersteds, the frequency at which ferromagnetic resonance occurs was estimated to be about 2200 mc/sec. This value is sufficiently far from our operating range (5,925–6,425 mc/sec) that we would expect a negligible loss contribution due to resonance absorption. This is confirmed by the low forward loss actually observed.

B. Ferrite Height

We have already pointed out that when the ferrite height is reduced from full height a more reasonable VSWR is obtained. This is due to the fact that we have relieved the stringent boundary requirements at the

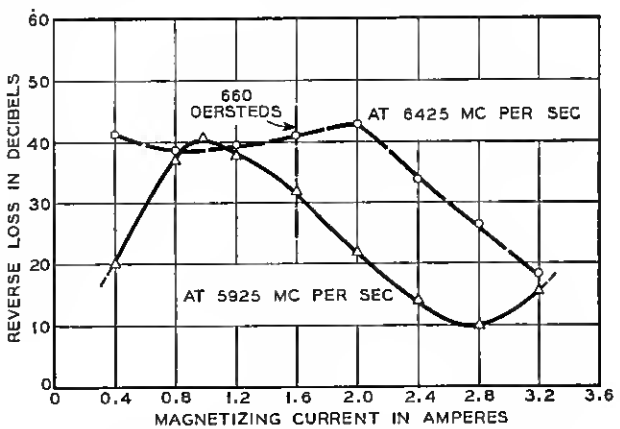

Fig. 8 — Reverse loss versus magnetizing current.

top and bottom faces of the ferrite and approach, in a sense, a less critical rod type geometry. A ferrite height of 0.550″ gave a VSWR $\sim$ 1.05 over the band. With full height slabs (0.795″), VSWR values as high as 10:1 have been observed for typical geometries.

C. δ and b

Experimentally, we have examined various ferrite thicknesses at different distances from the sidewall until optimum broadband performauce was obtained. Table I shows the ferrite distance from the wall which gave the best experimental results (bighest broadband ratios, low forward loss, high reverse loss) for each thickness δ of one of the BTL materials. It is interesting to note that the empirical quantity $\delta + b/2 -$

TABLE I

δ (mils)	b (mils)	$\delta + \frac{b}{2}$ (mils)	t (mils)	$\delta + \frac{b}{2} - 2t$ (mils)
201	11	206.5	3	200.5
189	35	206.5	3	200.5
186	42	207.0	3	201.0
176	65	208.5	3	202.5
189	42	210.0	6	198.0

$2t$, where t is the thickness of the resistive coating, is very nearly constant (within a few mils) for tbe stated range of δ and for this type of design.*

In Section IV a theoretical calculation using the null condition at 6175 mc/sec for a full height ferrite gives

$$\delta = 180 \text{ mils}$$

$$\text{b} = 38.7 \text{ mils}$$

so that $\delta + b/2 = 199.3$ mils. In the theoretical case t is assumed to be very small. It will be noted that the theoretical result for $\delta + b/2$ (with small t) agrees quite well witb the experimental $\delta + b/2 - 2t$. The question of the possible physical significance of tbis quantity is being investigated.

D. Placement of Resistance Material and Choice of Resistivity

The propagating mode with a full beight ferrite slab is of a TE_0 variety, the zero subscript indicating that no variation occurs with re-

* In one design of the isolator we used a General Ceramics magnesium manganese ferrite with $\delta = 0.180''$, $b = 0.074''$ and $t = 0.009''$ so that $\delta + b/2 - 2t = 199$ mils, in good agreement with Table I.

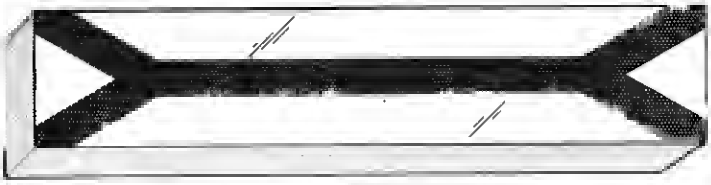

Fig. 9 — Distribution of small tangential electric fields at interior ferrite face.

Fig. 10 — Resistance configuration.

spect to height. A field null in this construction therefore extends across the entire face of the full height ferrite and all of this face is then "active" in the construction of an isolator. This field situation no longer accurately applies to the partial height slab. The departure of the ferrite from the top wall creates large fringing fields extending from the ferrite edges, and large electric fields may exist tangential to the ferrite face close to these edges. We would therefore expect the null condition to persist only in a small region about the vertical center of the ferrite face. We may, however, also expect longitudinally fringing modes (TM-like) to be scattered at the input edge of the ferrite slab so that a longitudinal field maximum will exist at the central region of the ferrite. However, this is a higher mode, so that this maximum decays rapidly past the leading edge.

Considering all the effects, the distribution of small tangential electric fields at the ferrite face may be expected to appear as shown in Fig. 9. Experimentally, we have utilized this low loss region and have avoided the decay region of the higher TM-like modes by using the resistance configuration shown in Fig. 10. The resistivity is uniform and about 75

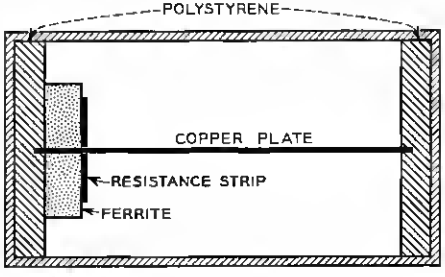

Fig. 11 — Elimination of longitudinal components.

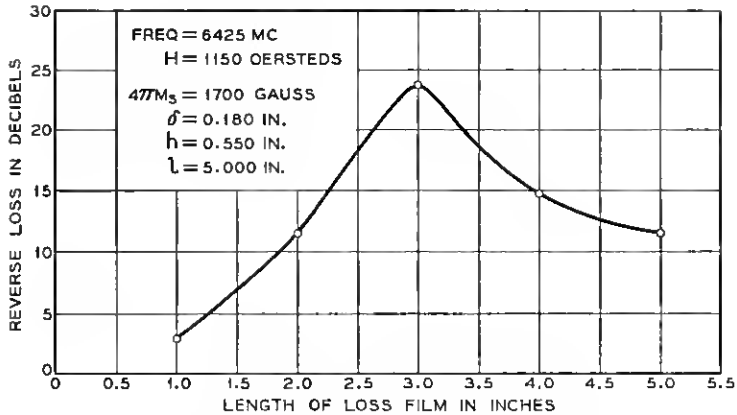

Fig. 12 — Attenuation versus length of resistance strip.

ohms/square. Variations of about ±30 ohms/square about this value result in little deterioration in performance.

Some further discussion of the perturbed dominant mode is of interest. We may think of the height reduction as primarily a dielectric discontinuity where we have effectively added a negative electric dipole density to a full height slab. Since this addition is smaller for the forward case (where there was initially a small electric field) than for the reverse case, we may expect the longitudinal components to be smaller for the forward propagating mode. The other type of longitudinal electric field,

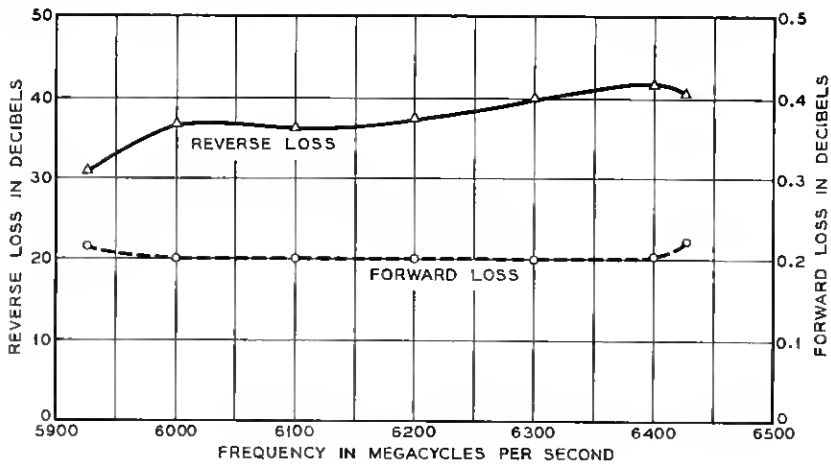

Fig. 13 — Loss versus frequency.

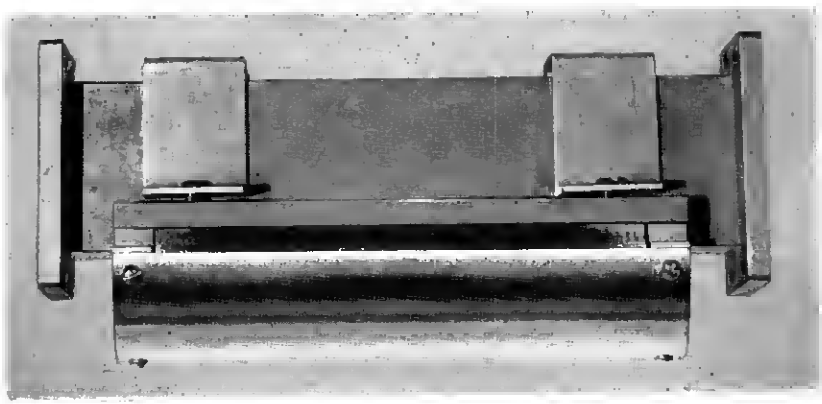

Fig. 14 — Isolator model.

which occurs due to the scattering of the TM-like longitudinal modes. decays rapidly and is not of consequence in an experiment now to be described. This experiment was designed to demonstrate the nonreciprocal nature of the longitudinal electric fields associated with the distorted dominant mode. It also shows that the existence of these components is significant as a loss mechanism for the reverse direction of propagation in the isolator. The geometry employed is shown in Fig. 11.

The copper plate was inserted to minimize longitudinal electric field components, and we may therefore expect to obtain less reverse loss than in the condition of its absence. The result of this experiment was that the reverse loss decreased from about 25 db* without the plate to 18 db with the plate. The forward loss was unaffected.

E. Determination of Length

Given a dominant mode distribution in a waveguide, attenuation will be a linear function of length, once this mode has been established. Consequently, one would expect that doubling the loss film length would double the isolator reverse loss. The isolator does not exhibit this behavior, however, as is illustrated in Fig. 12.

This occurrence might be explained by the appearance of still another longitudinal mode, peculiar in form to gyromagnetic media alone, which propagates simultaneously with the transverse electric mode, and is essentially uncoupled to the loss material. The maximum reverse loss

* This experiment was conducted with a different ferrite than that employed in the eventual design.

thus obtainable is limited by the scattering into this mode. The character of these singular modes will he discussed in a subsequent paper.

Results

The performance of the isolator as a function of frequency is shown in Fig. 13. Fig. 14 shows a completed model of the isolator.

IV. FURTHER ANALYSIS

While an exact characteristic equation is ohtainable for the overall geometry of the full height isolator, including the lossy film, the expressions which result are sufficiently complex to be all but impossihle to handle. However, if the resistance film is chosen to have small conductivity we may utilize a simple perturbation approach in which the field at the ferrite face is assumed to be unaffected by the presence of the loss film. A quantity η may then be defined* so that

$$\eta = \frac{|E_R|^2}{P} \qquad \text{(IV — 1)}$$

For small conductance values η is proportional to attenuation to first order in either direction of propagation. E_R, in equation (IV — 1), is the electric field adjacent to the film and P is the power flowing across the guide cross section. The loss in the ferrite material is not taken into account in this approximation, but it would naturally have a deteriorating effect on the isolator characteristics.

The ratio of the values of η corresponding to hackward and forward direction of propagation defines the isolation ratio, given in db/db, for the limit of very small conductivity.

Fig. 15 shows a calculated curve of the forward value of η and Fig. 16 shows the backward case. The isolation ratio shown in Fig. 17 demonstrates surprisingly large bandwidth for values of the order of 200 db/db. Fig. 18 portrays propagation characteritics for both forward and hackward power flows and provides the interesting observation, in conjunction with Fig. 16, that peak reverse loss occurs in the neighborhood of $\lambda = \lambda_g$.

Fig. 19 is a plot of α_1, the transverse wave numher, over the frequency range. The flatness of the forward wave number means that the position of null moves very little with frequency across the band. Hence the lossless transmission in the forward direction is broadband. Since the forward and backward wave numbers have such radically different

* See Appendix

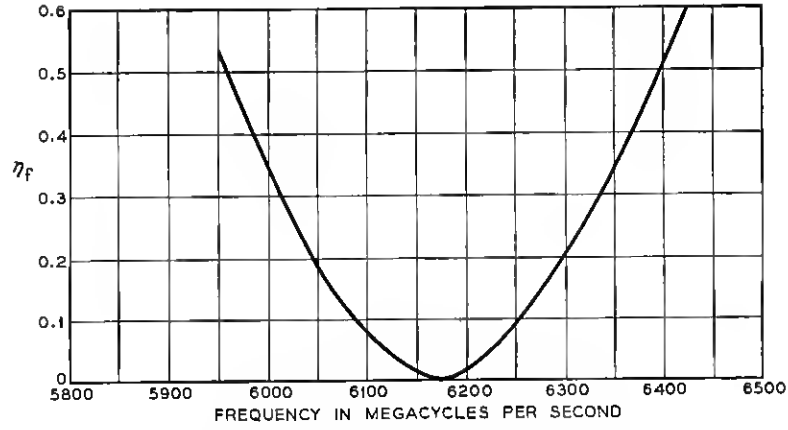

Fig. 15 — Relative attenuation — forward direction

rates of variation, a simple adjustment of parameters may be made to cause the forward null and maximum reverse attentuation to appear at the same frequency, resulting in an optimum performance.

The occurrence of the reverse maximum loss in the region of $\lambda = \lambda_g$ may roughly be explained as follows. As the transverse air wave number decreases, the admittance of the guide, defined on a power flow basis, increases. The electric field magnitude distribution must therefore generally decrease in such a fashion as to cause the overall power flow to re-

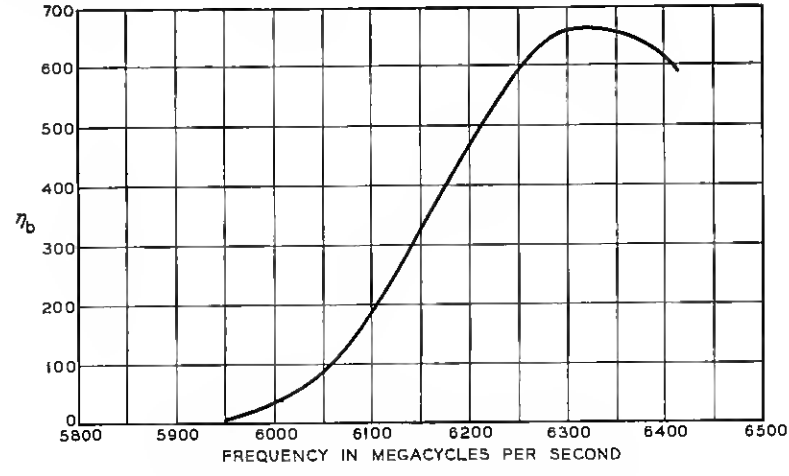

Fig. 16 — Relative attenuation — backward direction

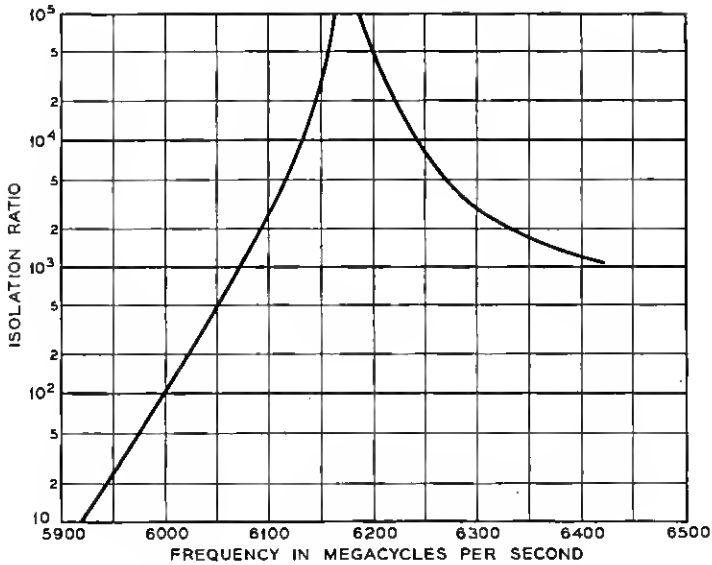

Fig. 17 — Ideal isolation characteristics.

main constant. On the other hand as the transverse air wave number decreases through real values, the electric field adjacent to the ferrite becomes relatively large. At $\lambda = \lambda_g$ the distribution is linear with relatively large dissipation at the ferrite face. As the transverse air wave number increases through imaginary values the distribution becomes exponential such that the field adjacent to the ferrite is always the maximum for the air region and the growth of the field at the face of the ferrite would not seem to be so great as formerly. One would therefore expect a maximum reverse loss somewhere in the region $\lambda = \lambda_g$.

The above considerations plus the transcendental equation for the null show consistency with the experimental design values which were:

$$\delta = 0.180''$$

$$L = 1.59$$

$$4\pi M_S = 1{,}700 \text{ gauss}$$

Using $H_{DC} = 600$ oersteds in the calculation we obtain the spacing from the guide wall $b = 0.0387''$. The fact that we used 600 oersteds for the full height slab calculation as opposed to the internal field of 300 oersteds found experimentally for the partial height slab should not be a source of confusion. It has been indicated earlier that the peak reverse loss shifts

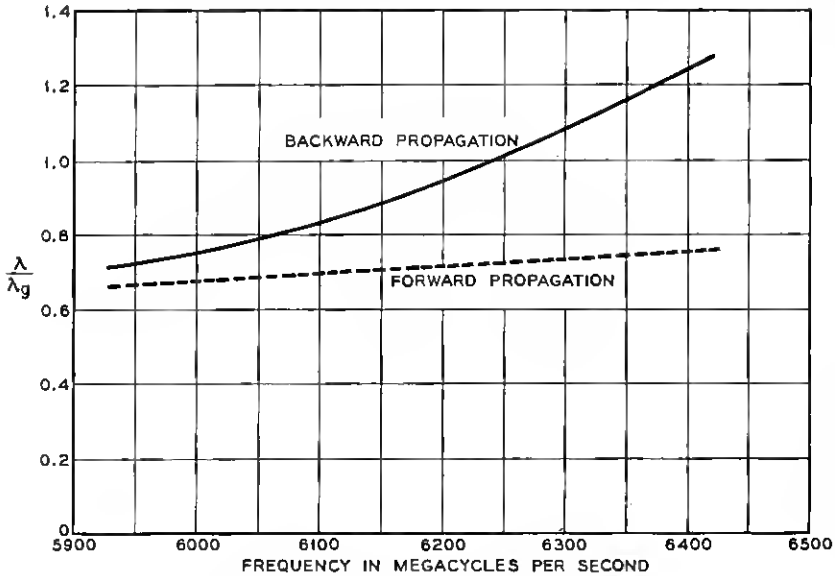

Fig. 18 — Ferrite isolator characteristics.

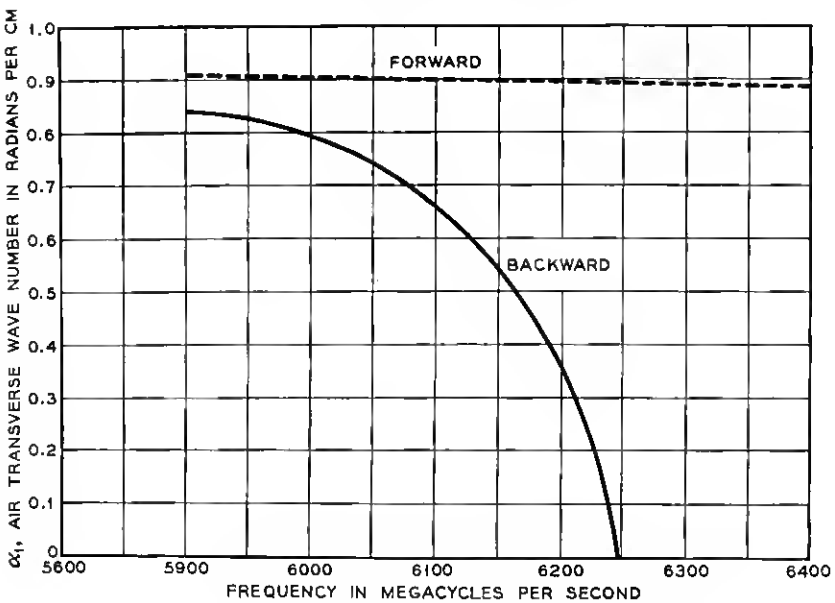

Fig. 19 — Transverse characteristics of a ferrite isolator

with ferrite height reduction. It is not inconsistent therefore to choose 600 oersteds for the full height analysis in contrast to the value determined from the experiment.

V. SCALING

Once the optimum set of parameters has been decided upon for a given frequency range (e.g., 5,925–6,425 mc/sec, $\delta = 0.180''$, $b = 0.074''$, $\ell = 5''$, $h = 0.550''$, $4\pi M_S = 1{,}700$ gauss, $H_{DC} = 660$ oersteds) it is a simple matter to scale these parameters to other frequency ranges. From Maxwell's equations:

$$\text{Curl } H = i\omega\varepsilon E + gE$$

$$\text{Curl } E = -i\omega T \cdot H$$

where T is the permeability tensor, and g is the conductivity in mhos/meter. The first of Maxwell's equations suggest that frequency scaling may be accomplished by permitting both the curl and the conductance to grow linearly with respect to frequency. The curl, which is a spatial derivative operator, may be made to increase appropriately by sbrinking all dimensions by a $1/\omega$ factor, which will keep the field configuration the same in the new scale.

Having imposed this condition on the first equation we must satisfy the second of Maxwell's equations by causing T to remain unchanged with frequency. T is a tensor given as follows for a cartesian coordinate system:

$$T = \begin{pmatrix} \mu_r & ik_r & 0 \\ -ik_r & \mu_r & 0 \\ 0 & 0 & 1 \end{pmatrix} \qquad \text{(V — 1)}$$

for a magnetizing field in the z direction. The components may be expanded in the following fashion:

$$\mu_r = \frac{1 + 4\pi\left(\frac{\gamma M_S}{\omega}\right)\left(\frac{\gamma H}{\omega}\right)}{\left(\frac{\gamma H}{\omega}\right)^2 - 1}$$

$$k_r = \frac{4\pi\left(\frac{\gamma M_S}{\omega}\right)}{\left(\frac{\gamma H}{\omega}\right)^2 - 1} \qquad \text{(V — 2)}$$

where $4\pi M_s$ is the saturation magnetization in gauss and γ is the magnetomechanical ratio. The Polder tensor evidently remains unchanged if M_s and H are both scaled directly with frequency.

Since the field distributions are assumed unchanged relative to the scale shift, normal and tangential E and H field components continue to satisfy the appropriate boundary equalities at interfaces. Then, invoking the uniqueness theorem, the guide characteristics are only as presumed and the model has been properly scaled as a function of frequency.

The scaling equations are:

$$\begin{aligned} d_1 &= \frac{\omega_2}{\omega_1} d_2 \\ g_1 &= \frac{\omega_1}{\omega_2} g_2 \\ M_{s_1} &= \frac{\omega_1}{\omega_2} M_{s_2} \\ (H_0)_1 &= \frac{\omega_1}{\omega_2} (H_0)_2 \end{aligned} \qquad \text{(V—3)}$$

where d is any linear dimension.

CONCLUSION

An isolator with low forward loss and high reverse loss can be constructed by a proper choice of parameters. Once a suitable design has been reached the scaling technique can be used to reach a suitable design for other frequencies.

As yet, a theoretical analysis of this problem has been carried out only for a full height ferrite.

ACKNOWLEDGMENT

We would like to thank F. J. Sansalone for his assistance in developing the field displacement isolator. We would also like to thank Miss M. J. Brannen for her competent handling of the numerical computations.

APPENDIX

It is desirable to establish an isolator figure of merit. A simple quantity characterizing the isolator action is the normalized rate of power

loss in the resistive strip, for an idealized ferrite, in the low conductive limit of such a strip. Let

$$\eta = \frac{|E_r|^2}{P}$$

where η is the appropriate quantity, E_r is the field at the resistance, and P is the total power flow across the guide cross-section. This figure of merit is related to the rate of change of the attenuation constant (A) with respect to strip conductance in the following manner:

$$\frac{dA}{dg} = 0.04343\eta h \text{ (dh)(ohms)/cm}$$

where h is the fractional height of the loss strip, and g is the reciprocal of the surface resistivity in ohms/square.

The total power flow may he divided into integrations of the Poynting vector over the three regions of the guide cross-section. The following results are ohtained normalized to $E_r = \sin \alpha_1 a$:

Region 1: $0 \leqq x \leqq a$

$$P_y^{(1)} = \frac{\beta}{2\omega\mu_0}\left(a - \frac{\sin 2\alpha_1 a}{2\alpha_1}\right)$$

Region 2: $a \leqq x \leqq a + \delta$

$$P_y^{(2)} = \frac{\beta}{2\omega\mu_0}\left(\frac{\mu_r\delta}{\mu_r^2 - k_r^2}(d_1^2 + d_2^2) + \frac{\sin 2\alpha_2\delta}{2\alpha_2(\mu_r^2 - k_r^2)} \cdot\left[\mu_r(d_1^2 - d_2^2) - \frac{k_r}{\beta}\alpha_2(2d_1d_2)\right] + \frac{1 - \cos 2\alpha_2\delta}{2\alpha_2(\mu_r^2 - k_r^2)} \cdot\left[\mu_r(2d_1d_2) + \frac{k_r\alpha_2}{\beta}(d_1^2 - d_2^2)\right]\right)$$

Region 3: $a + \delta \leqq x \leqq L$

$$P_y^{(3)} = \frac{\beta}{2\omega\mu_0}\left(b - \frac{\sin 2\,\alpha_1 b}{2\alpha_1}\right)\left(\frac{d_1 \cos \alpha_2\delta + d_2 \sin \alpha_2\delta}{\sin \alpha_1 b}\right)^2$$

where $$d_1 = \sin \alpha_1 a$$

and

$$d_2 = \frac{1}{\mu_r\alpha_2}[(\mu_r^2 - k_r^2)\alpha_1 \cos \alpha_1 a + k_r\beta \sin \alpha_1 a]$$

BIBLIOGRAPHY

1. Tellegen, B. D. H., Philips Res. Rep., **3**, 1948.
2. Hogan, C. L., B.S.T.J. **31**, 1952.
3. Fox, A. G., Miller, S. E., and Weiss, M. T., B.S.T.J. **34**, p. 5., Jan. 1955.
4. Turner, E. H., URSI Michigan Symposium on Electromagnetic Theory, June, 1955.
5. Polder, D., Phil. Mag., **40**, 1949.
6. Lax, B., Button, K. J., Roth, L. M., Tech Memo No. 49, M.I.T. Lincoln Laboratory, Nov. 2, 1953.
7. Kittel, C., Phys. Rev., **73**, 1948.